Structure
Article

Substrate Recognition Mechanism of Atypical Protein Kinase Cs Revealed by the Structure of PKCι in Complex with a Substrate Peptide from Par-3

Chihao Wang,[1,3] Yuan Shang,[1,3] Jiang Yu,[1,4] and Mingjie Zhang[1,2,*]
[1]Division of Life Science, State Key Laboratory of Molecular Neuroscience
[2]Institute for Advance Study
Hong Kong University of Science and Technology, Clear Water Bay, Kowloon, Hong Kong
[3]These authors contributed equally to this work
[4]Present address: School of Physics, The University of New South Wales, Sydney NSW 2052, Australia
*Correspondence: mzhang@ust.hk
DOI 10.1016/j.str.2012.02.022

SUMMARY

Protein kinase C (PKC) play critical roles in many cellular functions including differentiation, proliferation, growth, and survival. However, the molecular bases governing PKC's substrate recognitions remain poorly understood. Here we determined the structure of PKCι in complex with a peptide from Par-3 at 2.4 Å. PKCι in the complex adopts catalytically competent, closed conformation without phosphorylation of Thr402 in the activation loop. The Par-3 peptide binds to an elongated groove formed by the N- and C-lobes of the kinase domain. The PKCι/Par-3 complex structure, together with extensive biochemical studies, reveals a set of substrate recognition sites common to all PKC isozymes as well as a hydrophobic pocket unique to aPKC. A consensus aPKC's substrate recognition sequence pattern can be readily identified based on the complex structure. Finally, we demonstrate that the pseudosubstrate sequence of PKCι resembles its substrate sequence, directly binds to and inhibits the activity of the kinase.

INTRODUCTION

Protein kinase C (PKC) family of serine/threonine kinases plays essential roles in multiple signaling pathways and cellular processes including early development, tumor formation and progression, immune responses, and cell polarity regulation (Henrique and Schweisguth, 2003; Kalive et al., 2010; Martiny-Baron and Fabbro, 2007; Tan and Parker, 2003; Webb et al., 2000). Every PKC isozyme contains N-terminal regulatory regions and a C-terminal kinase domain. Based on their structures and regulatory mechanism, PKCs can be divided into conventional, novel and atypical subfamilies (cPKC, nPKC, and aPKC, respectively). Each cPKC (α, β1, β2, and γ) contains two diacylglycerol-binding C1 domains (C1A and C1B) followed by a Ca^{2+}- and phosphoinositol lipid-binding C2 domain in their N-terminal regulatory domains. Members of nPKCs (δ, θ, η, ε) have the same domain compositions in their regulatory region as cPKCs do, except that the C2 domain of each nPKCs is located N-terminal to the two C1 domains, and the C2 domains of nPKCs do not bind to Ca^{2+} (Ponting and Parker, 1996). In contrast to the cPKCs and nPKCs, aPKC isozymes (ζ and λ/ι) do not contain C2 domain. Instead, each aPKC contains a PB1 domain at the very N-terminus followed by an atypical C1 domain that does not bind to DAG (Suzuki et al., 2003). Additionally, all PKCs contain a pseudosubstrate sequence in their N-terminal regulatory domains, which maintains kinases in their inactive state in the absence of activation signals (House and Kemp, 1987; Newton, 1997). Members of both the cPKCs and nPKC families require second messengers (DAG and/or Ca^{2+}) for their activations (Webb et al., 2000). In contrast, PKCζ and PKCι require neither Ca^{2+} nor DAG for their activation, and hence they are termed as atypical PKCs. PKCζ and PKCι share very high amino acid sequence identity. Compared to PKCζ, PKCι is ubiquitously expressed in all tissues (Fields and Regala, 2007). The majority of studies on aPKC described in the literature are on PKCι. Despite of their critical roles in many biological processes including asymmetric cell division, cell polarity establishment and maintenance, cell migration, and tumor formation (Etienne-Manneville and Hall, 2003; Fields and Regala, 2007; Prehoda, 2009), the activation mechanisms of PKCζ and PKCι are poorly understood.

Besides being regulated by the secondary messengers via the N-terminal regulatory domains, PKCs are also regulated through phosphorylation of Ser/Thr residues in the activation loop, the turn-, and the hydrophobic-motifs in their C-terminal regulatory segments (Newton, 2003). The activation loop of PKC isoforms has been shown to be phosphorylated by PDK1 and this phosphorylation primes PKCs for further autophosphorylation and activation (Behn-Krappa and Newton, 1999; Le Good et al., 1998). For atypical PKCs, the phosphorylation site in the hydrophobic motif is replaced by a glutamic acid, which presumably mimics the corresponding phosphor-Ser/Thr in other PKCs. Previously reported aPKC kinase structures were obtained with both the activation loop and turn-motif Ser/Thr phosphorylated (Messerschmidt et al., 2005; Takimura et al., 2010). However, it has been shown that phosphorylation of the Thr residue in the activation loop is not required for PKCζ's kinase activity (Ranganathan et al., 2007). Consistent with this finding and to the best of our knowledge, it has not been reported

that, at least in the Par-3/Par-6/aPKC-mediated cell polarity regulations, aPKC requires another upstream kinase for its activation. Again, it is unclear why aPKCs do not require activation loop phosphorylation for their activation.

In line with the remarkable range of biological functions regulated by PKCs, numerous proteins, such as GSK3β, MARCKS, LGN, Par-3, Lgl, Crumb, etc., are known as direct substrates of the kinases (Betschinger et al., 2003; Goode et al., 1992; Hao et al., 2010; Herget et al., 1995; Nagai-Tamai et al., 2002; Sotillos et al., 2004). Not matched with the extensive functional and biochemical studies of PKC-mediated phosphorylation of target proteins, no structure has been reported for any member of PKCs in complex with a substrate protein/peptide to date; although the structures of the kinase domains of a number of PKC isoforms as well as the full-length PKCβII have been solved (Grodsky et al., 2006; Leonard et al., 2011; Messerschmidt et al., 2005; Takimura et al., 2010; Wagner et al., 2009; Xu et al., 2004). Our current understandings of the substrate specificity of PKC isozymes are largely derived from an oriented peptide library study nearly 15 years ago (Nishikawa et al., 1997). High resolution atomic structures of PKCs in complex with their cognate substrates will be highly valuable to enhance our knowledge of the substrate recognition mechanisms of different isoforms of PKCs.

Here we present the structure of the PKCι kinase domain in complex with a substrate peptide derived from Par-3, which, to our knowledge, represents the first substrate-bound structure of the entire PKC family kinases. The structure of the PKCι/Par-3 peptide complex reveals that the kinase domain adopts an active conformation even though Thr402 in the activation loop is not phosphorylated. The Par-3 peptide binds to the groove between the N- and C-lobes of the kinase via combined hydrophobic and charge-charge interactions. The structure of the complex, along with detailed amino acid sequence analysis and extensive biochemical studies, allowed us to derive a consensus and specific substrate sequence for aPKC. The data presented in this study can also serve as a template in understanding substrate specificities of other members of PKC isozymes.

RESULTS

aPKCι Binds and Phosphorylates a Short Peptide Fragment of Par-3

Previous studies reported that Par-3 can be phosphorylated by aPKC. The aPKC phosphorylation site is located within amino acid residues 712–936, and the region is thus referred to as the aPKC binding domain of Par-3 (Morais-de-Sá et al., 2010; Nagai-Tamai et al., 2002). To characterize the aPKC/Par-3 interaction in detail, we mapped the minimal aPKC binding domain of Par-3 using bacterially purified GST-fused Par-3 fragments to pull down GFP-PKCι kinase domain (aa 222–586 of mouse PKCι) expressed in HEK293 cells (Figure 1). This mapping experiment revealed that a 28-residue fragment of Par-3 (aa 813–840) is sufficient to bind to the kinase domain of PKCι (Figure 1A). Correspondingly, any Par-3 sequences containing this 28-residue peptide fragment can be robustly phosphorylated by the purified GFP-PKCι kinase domain (Figure 1B). This minimal PKCι-binding sequence of Par-3 contains 2 Ser residues (Ser827 and Ser829) that are completely conserved from worm to mammals (Figures 1C and 1E). Substitution of Ser829 with Ala has minimal impact on its phosphorylation by PKCι. In contrast, substitution of Ser827 with Ala largely eliminated its PKCι-mediated phosphorylation (Figure 1B, lane 4), indicating that Ser827 is the main PKCι phosphorylation site of the Par-3 fragment. Replacements of both Ser827&829 with Ala eliminated PKCι-mediated phosphorylation of the Par-3 fragment (Figure 1B). Only background level of phosphorylation could be detected for the longest Par-3 fragment (aa 712–854) when a kinase-dead mutant of PKCι, in which the catalytic Lys273 was replaced by Arg (K273R-PKCι), was used for the phosphorylation assay (Figure 1B, last lane), indicating that the phosphorylation of the Par-3 fragments shown in Figure 1B are specifically catalyzed by PKCι.

We found that substitution of Ser827 with Glu essentially abolished Par-3's binding to PKCι (Figure 1D), indicating that phosphorylation promotes substrate dissociation from the kinase. This result provides a mechanistic explanation to well-documented findings showing that aPKC-mediated phosphorylation of Par-3 (or Bazooka in *Drosophila*) promotes Par-3's dissociation from the Par-6/aPKC complex at the apical membranes of polarized epithelia (Morais-de-Sá et al., 2010; Nagai-Tamai et al., 2002). The substitution of Ser827 with Ala also weakened the Par-3 fragment's binding to PKCι, suggesting that the side chain of Ser827 also plays a positive role in the kinase binding. In contrast, substitution of Ser829 with Ala has no detectable impact on Par-3's binding to PKCι. It is noted that substitution of Ser829 with Glu also eliminated Par-3's binding to PKCι (Figure 1D), although it is not clear what does this mean at the current stage.

Overall Structure of the PKCι/Par-3 Peptide Complex

To elucidate how PKCι binds to Par-3, we determined the crystal structure of the K273R-PKCι kinase domain in complex with the 28-residue Par-3 peptide (^{813}DPVLAFQREGFGRQSMSE KRTKQFSNAS^{840}) and an ATP analog AMP-PCP (referred to as the PKCι/Par-3 complex from hereafter) at 2.4 Å resolution (Table 1). The Lys273 to Arg mutation should inactivate the kinase activity of PKCι with minimal structural perturbations. Except for a few negatively charged residues in the loop connecting αB and αC (^{282}DDED^{285} to be specific) and a short fragment proceeding αG (^{449}SDNPDQ^{454}), the entire kinase domain is well resolved in the refined model of the PKCι/Par-3 complex (Figure 2A). The kinase domain is composed of an N-lobe, a C-lobe, and a regulatory segment composed of a turn-motif and a hydrophobic motif at the C-terminal tail, which turns back from the C-lobe and wraps around the N-lobe. Thr554 in the turn motif of the regulatory segment is phosphorylated (Figure 2A). In the crystal, only the adenosine ring of AMP-PCP is defined (Figure 2A). The overall structure of the PKCι kinase domain determined here is highly similar to the human PKCι kinase domain either in complex with ATP or an ATP analog-based inhibitor (Messerschmidt et al., 2005; Takimura et al., 2010), thus we will not discuss the structural features that are shared by these three structures in any details further. A unique exception found in the PKCι/Par-3 complex is that Thr402 in the activation loop of the kinase is not phosphorylated, and yet the conformation of the loop is well-defined (Figures 2A and 3;

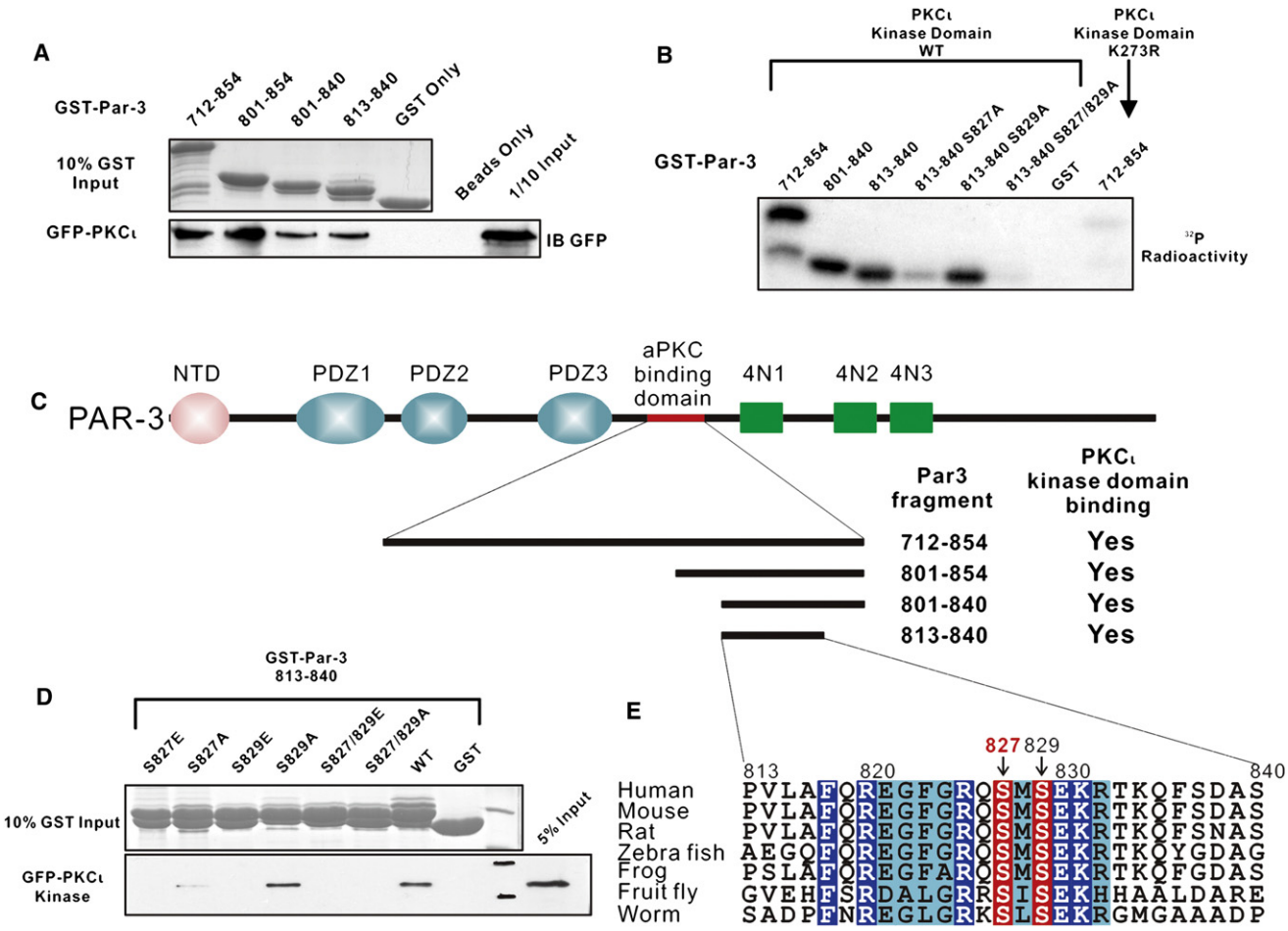

Figure 1. PKCι Binds to and Phosphorylates a 28-Residue Peptide Fragment of Par-3

(A) Mapping of the minimal PKCι binding region of Par-3. Purified GST-fused Par-3 fragments were used to pull-down GFP-PKCι kinase domain expressed in HEK293T cells. GST-Par-3 proteins were stained by Coomassie blue, and GFP-PKCι was detected with anti-GFP antibody.

(B) Purified PKCι kinase domain specifically phosphorylates Ser827 of Par-3 in ^{32}P-autoradiography-based assays. The kinase-dead mutant, K273R-PKCι, is used as the negative control of the experiment.

(C) Schematic diagram showing the domain organizations of Par-3 as well as the various Par-3 fragments used in (A).

(D) Phospho-mimetic substitution of Ser827 with Glu abolishes Par-3's binding to PKCι.

(E) Alignment of the 27-residue, PKCι binding sequence of Par-3 from different species. The two serine residues in these sequences are colored in red, the fully conserved residues are colored in blue, and highly conserved residues are highlighted in cyan.

Figures S3A and S3B available online). A total of 16 residues of the Par-3 peptide (^{814}PVLAFQREGFGRQSMS^{829}) are clearly defined (Figures 2A and 4A). The Par-3 peptide binds to the predicted substrate binding groove formed by the N- and C-lobe of the kinase in a rather twisted conformation due to the formation of two turn-like structures (Figure 2A, see Figure 4 and related discussions below).

PKCι Kinase Domain Adopts a Closed Conformation in the Complex

Based on the relative positions of the N-lobe to the C-lobe, the overall conformation of a kinase can be classified as either the open state or the closed state, each representing different steps in its catalytic cycle (Taylor and Kornev, 2011). In its open state, a kinase can recruit ATP to its N-lobe for another cycle of catalytic reaction. Whereas in the closed state, the "closure" of the N- and C-lobes positions ATP as well as the catalytic amino acids in a geometry suitable for transferring γ-phosphate from ATP to its substrate (Johnson et al., 2001). We superimposed the C-lobes of PKCι structure from this study with that of the open state PKCι structure (Protein Data Bank [PDB] code: 3A8W) determined earlier (Takimura et al., 2010), and found that the N-lobes of the two structures have an root-mean-square deviation (rmsd) value of ~3.45 Å (Figure 2B). In contrast, the rmsd value of only ~1.24 Å was found for the N-lobes when the C-lobe of the PKCι structure from this study was superimposed with that of the closed state of PKCθ (PDB code: 1XJD) (Figure 2B). This structural analysis indicates the PKCι kinase domain in complex with Par-3 adopts a closed conformation (Figure 2B). A rigid body rotation of the N-lobe by ~15° clockwise would convert aPKC from the open- to the closed-conformation (Figure 2B). In the open state, the γ-phosphate of ATP would be

Table 1. Statistics of Data Collection and Model Refinement of the PKCι/Par-3 Peptide Complex

Data Collection	
Data sets	PKCι /Par-3
Source	SSRF-BL17U
Space group	C2
Unit cell parameters (Å,°)	a = 101.5, b = 54.9, c = 82.5, β = 115.2
Resolution range (Å)[a]	50.00–2.40 (2.44–2.40)
No. of unique reflections[a]	14,458 (726)
Redundancy[a]	2.9 (2.8)
I/s[a]	11.4 (1.68)
Completeness (%)[a]	87.8 (90.1)
R_{merge} (%)[a,b]	8.4 (56.7)
Structure refinement	
Resolution (Å)[a]	21.2–2.40 (2.59–2.40)
R_{cryst}/R_{free} (%)[a,c,d]	17.2 (21.4)/24.1(29.9)
Rmsd bonds (Å)/angles (°)	0.008/1.132
No. of reflections	
Working set	13,400
Test set	659
Protein/peptide/other atoms	2,564/122/70
B-factor of protein/peptide[e]	43.72/38.79
Ramachandran plot	
Most favored regions (%)	96.4
Additionally allowed (%)	3.3
Outliers (%)	0.3

Rmsd, root-mean-square deviation.
[a]Numbers in parentheses represent the value for the high resolution shell.
[b]R_{merge} = SUM (ABS(I − <I>))/SUM (I), where I is the intensity of measured reflection and <I> is the mean intensity of all symmetry-related reflections.
[c]$R_{cryst} = \Sigma|F_{calc} - F_{obs}|/\Sigma F_{obs}$, where F_{obs} and F_{calc} are observed and calculated structure factors.
[d]$R_{free} = \Sigma_T|F_{calc} - F_{obs}|/\Sigma F_{obs}$, where T is a test data set of ~5% of the total unique reflections randomly chosen and set aside prior to refinement.
[e]Refinement is processed with phenix.refinement, and B-factor values are extracted by phenix validation tools.

far away from Asn373 (~5.2 Å) and Lys370 (~6.1 Å) in the catalytic loop, and from Ser827 (~7.1 Å to the phosphate-accepting oxygen atom) of the Par-3 peptide (Figures S2A and S2B). Closure of the N-lobe positions the ATP γ-phosphate at the catalytically competent position both with respect to the catalytic residues from the kinase and the phosphate accepting Ser827 of Par-3 (Figures S2C and S2D). Taken together, the structure of the PKCι/Par-3 complex determined in this study reveals that the kinase domain is in its catalytically competent, closed conformation.

PKCι Is Active without the Activation Loop Phosphorylation

ABC kinases together with other kinases such as PKG all belong to the so called AGC kinases family as they share considerable similarities in their kinase domains (Pearce et al., 2010). Activation of AGC kinases generally requires phosphorylation of three Ser/Thr residues: one from the activation loop and two from the C-terminal regulatory segment composed of a turn motif and a hydrophobic motif. The phosphorylation of the turn motif and the hydrophobic motif anchors the regulatory segment to the N-lobe, which is critical for keeping the two lobes of the kinases in their active conformations (Pearce et al., 2010). In the PKCι/Par-3 complex, Thr554 in the turn motif is phosphorylated. Glu573 in the hydrophobic motif and phosphor-Thr554 in the turn motif function together to stabilize the interaction between the C-terminal regulatory segment and the N-lobe of the kinase domain (Figure S3D).

Phosphorylation of the activation loop shapes the substrate binding site and/or modulates the phosphate transfer step during catalysis, and is known as a general activation mechanism in the majority of protein kinases (Adams, 2003). In the PKCι/Par-3 complex, the entire activation loop is clearly defined and Thr402 in the activation loop is not phosphorylated (Figures S3A, S3B, and 2A). Although Thr402 is not phosphorylated, the conformation of the activation loop of PKCι in our structure (in yellow) is essentially identical to that of PKCι crystalized with Thr402 phosphorylated (in orange) (Messerschmidt et al., 2005) except for the several polar interactions induced by the phosphate group (Figure 3B). The formation of this well-defined activation loop conformation in the absence of Thr402 phosphorylation is the result of extensive hydrogen bonding networks, charge-charge interactions, and hydrophobic contacts between the residues from the activation loop and amino acids from both lobes of the kinase (Figure 3). The conserved "DFG"-motif ("^{386}DYG^{388}" in PKCι) (Figure 3A) and the "P+1"-pocket (Figure 3C) of the kinase domain also actively participate in the stabilization of the activation loop conformation. It is interesting to note that the hydrophobic residue corresponding to Phe422 in PKCι, which is in close contact with Leu394 and thus expected to play a positive role in stabilizing the activation loop conformation, is conserved only in aPKCs and PKCδ (Figure S1). In line with this observation, both aPKC and PKCδ have been reported to be catalytically active even when their activation loops are not phosphorylated (Stempka et al., 1997; Ranganathan et al., 2007). Our structural data indicate that the interaction between Par-3 and the kinase domain of PKCι does not require the phosphorylation of Thr402. Our structure-based analysis further suggests that activation of aPKCs may not require the phosphorylation of Thr in their activation loops.

Finally, the conformation of PKCι in the complex with Par-3 contains two prominent structural hallmarks known for many protein kinases in their active states, namely the formation of two spatially continuous hydrophobic interaction networks called the R-spine (regulatory spine) and the C-spine (catalytic spine) (see Figure S3E for details) (Kornev et al., 2008; Taylor and Kornev, 2011). The R-spine and the C-spine are linked by the gatekeeper Ile322 (the orange sphere, Figure S3E middle). Residues forming both the R-spine and the C-spine of PKCι are aligned well with the active forms of AGC kinases including ATP-bound apo-PKCι (PDB code: 3A8W), PKB in complex with a GSK peptide (PDB code: 1O6L), and PKCθ (PDB code: 1XJD) (Figure 3D). In contrast, the inactive PKB kinase domain (PDB code: 1GZN) has a misaligned R-spine and C-spine (Figure S3E).

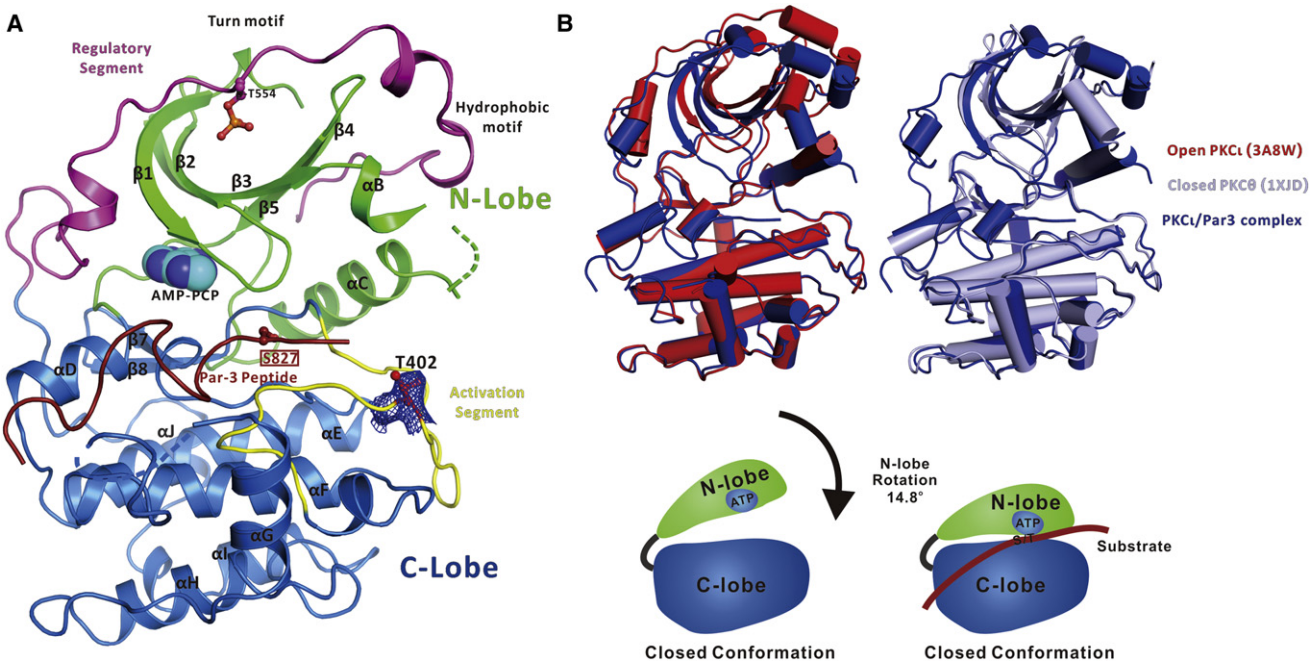

Figure 2. PKCι Adopts an Active and Closed Conformation in Complex with the Par-3 Peptide

(A) Ribbon diagram showing the overall structure of the PKCι/Par-3 complex. The ATP analog, AMPPCP, is shown in sphere and colored in cyan. Thr554 in the regulatory segment is phosphorylated and drawn in the stick model. The unphosphorylated Thr402 in the activation loop is also shown with the stick model. The 2Fo-Fc electron density of the unphosphorylated Thr402 in the activation loop contoured at 0.9σ is shown with meshed surface, colored in blue. The bound Par-3 peptide is shown with the worm model in scarlet red.

(B) Comparison of the overall kinase domain structure of PKCι from the PKCι/Par-3 complex with that of an open state PKCι (PDB code: 3A8W), and that of a closed state PKCθ (PDB code: 1XJD). In the comparison, the C-lobe of the kinase domains are superimposed with each other, and the positions of the N-lobes are compared. The cartoons below show the relative position of the N-lobe, C-lobe, substrate, and ATP in both the open and closed states of the kinases.

See also Figures S2 and S3.

The Kinase and Par-3 Peptide Interface

The Par-3 peptide occupies the groove between the N- and C-lobes of the kinase (Figure 4A). The kinase-bound peptide is twisted due to the formation of two continuous turn-like structures, which are facilitated by the presence of two Gly residues (Gly822 and Gly824) in the peptide (Figures 4B and 4C). The binding of the Par-3 peptide to PKCι is rather extensive, covering 965 Å^2 of surface area. Both polar (charge-charge and hydrogen bonding) and hydrophobic interactions contribute to the kinase/substrate binding (Figures 4B and 4C). Detailed analysis of the complex structure identifies three discrete hydrophobic interactions sites (referred to as the ψ-site-1, -2, and -3) and three charge-charge interaction sites (referred to as the charge site-1, -2, and -3) that are critical for binding to the Par-3 peptide (Figures 4B and 4C).

The ψ-site-1 is formed by the side chains of Met331, Met334 from αD, and Leu371 proceeding β7, and this site accommodates Phe818 at the −9 position of the Par-3 peptide. Ile445 and Val446 from the unique insertion between αF and αG found in aPKCs, and Leu460 from αG form the ψ-site-2, which functions as the binding site for Phe823 at the −4 position of the Par-3 peptide. The ψ-site-3 is formed by Phe403, Pro407, Ile410 from the P+1 loop, and Phe461 from αG, and this hydrophobic pocket accepts Met828 at the +1 position of the Par-3 peptide (Figures 4B and 4C).

The charge site-1 contains Asp329 N-terminal to αD, Asp372 before β7, and Asp543 before the turn-motif. Arg820 at the −7 position of the Par-3 peptide forms salt-bridges with the three negatively charged residues in the charge site-1. Asp435 from αF acts as the principle residue in the charge site-2 and forms a salt bridge with Arg825 at the −2 position of the Par-3 peptide. Additionally, the side chain of Arg825 forms several hydrogen bonds with side chains of Asn408 and Tyr409 from the P+1 loop of the kinase. The charge site-3 is rather tentative. We notice from the structure of the PKCι/Par-3 complex that a stretch of positively charge residues (e.g., Lys831 and Arg832 at the +4 and +5 positions that are not well-defined in the structure) of the Par-3 peptide are in close vicinity of a negatively charge cassette ("^{282}DDED^{285}") proceeding αC of the kinase (Figures 4C and S1). We hypothesize that the "^{282}DDED^{285}"-cassette forms the charge site-3 of the kinase, and this charge site interacts with Lys831 and Arg832 from the Par-3 peptide. Indeed, either mutation of K831 or R832 in the Par-3 peptide with Ala (Figure 4D) or substitution of "^{282}DDED^{285}" with "KLKQ" (the corresponding sequence in PKA, Figure S1) in the kinase domain largely decreased the binding between PKCι and the Par-3 peptide (Figure 4E). Further consistent with the above structural analysis, substitutions of Phe818, Arg820, Phe823, or Arg825 of the Par-3 peptide individually with Ala either

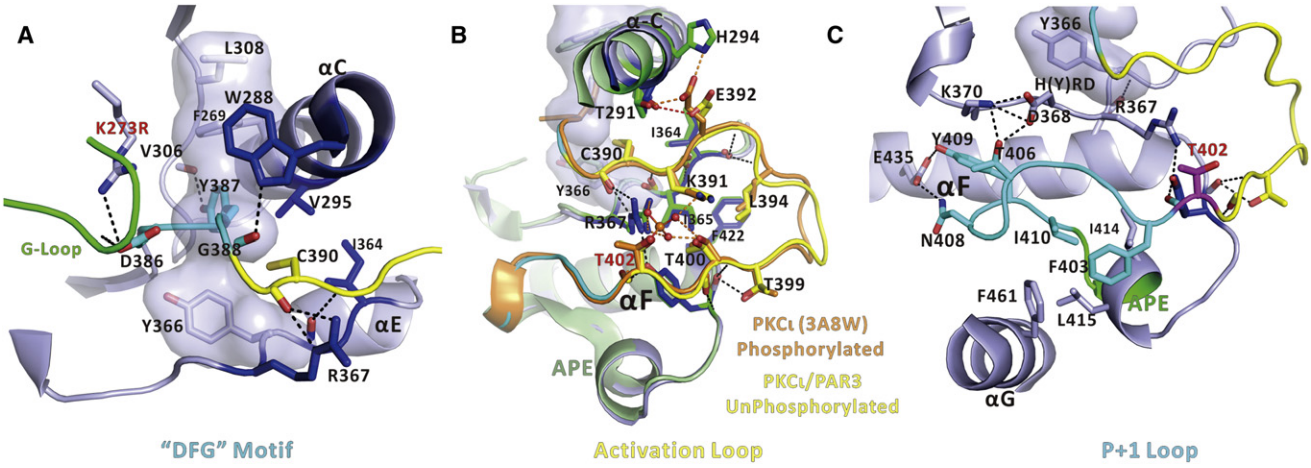

Figure 3. PKCι in the PKCι/Par-3 Complex Is Active without the Need of Its Activation Loop Phosphorylation

(A) The interactions with the "DFG"-loop of the kinase domain (colored in cyan) that helps to orientate the activation loop. The hydrogen bond between Y387 and the backbone of V306 is unique for aPKC isozymes (Figure S1).

(B) The superimposed structural comparison of the unphosphorylated activation loop of PKCι (in yellow) in the PKCι/Par-3 complex with that of the phosphorylated activation loop of PKCι (colored in orange). Numerous interactions that stabilize the unphosphorylated activation loop of PKCι. Expect for the polar interactions between the phosphate group and R367, K391, and T400, the rest of the interactions are retained in the unphosphorylated activation loop of the kinase.

(C) The interactions in "P+1" loop (colored in cyan) that helps to stabilize the activation loop. Two hydrogen bonding networks formed by N408-E435-Y409 and K370-T406-D368, together with the hydrophobic interactions formed by F403, I410, L415, and F461 in the "P+1" loop stabilize the conformation of the activation loop.

See also Figure S3.

abolished or largely weakened the peptide's binding to PKCι (Figure 4D). As a control, substitution of Gln826, whose side chain points to the opposite direction of the binding interface, with Ala had no effect on the peptide's binding to the kinase (Figure 4D).

A Consensus Sequence Pattern of aPKC Substrates

To further understand substrate specificities of aPKCs, we aligned the kinase domain sequences of ABC kinases (PKA, PKB, and PKC), and mapped the sequence conservation profile of the ABC kinases onto the PKCι structure determined in this work (Figure 5A). This sequence conservation map reveals the following features for the substrate binding surfaces of the ABC family kinases: the entire ABC family kinases share similar substrate binding surfaces; the surface similarity of the PKC subfamily is even greater; and finally, the substrate binding surfaces among aPKCs are completely conserved. With this finding, we predicted that we should be able to identify a consensus substrate recognition pattern for aPKCs based on the structure of the PKCι/Par-3 complex and other previously identified aPKC substrates including Numb (Smith et al., 2007), Lgl (Betschinger et al., 2003), and Crb3 (Sotillos et al., 2004).

Figure 5B is the amino acid sequence alignment of the Par-3 peptide with predicted aPKC's substrate peptides from Numb, Lgl, and Crb3. The alignment is first based on the Ser residues at the 0 position, and then aided by the two positively charged residues (Arg820 and Arg825 in Par-3) binding to the charge site-1 and -2 and the two hydrophobic residues (Phe818 and Phe823 in Par-3) binding to the ψ-site-1 and -2 of PKCι shown in Figure 4. Based on this alignment analysis, a highly consensus aPKC's substrate recognition sequence pattern emerges as:

$$\psi - X_{0-1} - R/K - X_{0-2} - \psi - A/G0 - 1_{0-1} - R/K - X - S/T(0) - \psi - X_{1-3} - R/K - R/K,$$

where "ψ" represents hydrophobic residues, and "X" denotes any residue but preferably polar amino acids. The presence of a Gly at the −3 position of the Par-3 peptide allows the formation of the Turn-2. Without this Gly, the Arg and the hydrophobic residue (Arg_{-2} and Phe_{-4} of the Par-3) can assume similar position if the backbone of the segment adopts an extended structure. Similarly, the positively charged residue in the −7 position of the Par-3 peptide (Arg820) is likely to be able to occupy a similar position even with the removal of Gly_{-5} and/or Glu_{-6} in Par-3, which forms the Turn-1 (Figures 5A and 5B). The above analysis provides an explanation to the variable gaps in the aPKC's substrate sequences shown in Figure 5B.

The structure and the sequence conservation map show that aPKCs contain a unique insertion with seven to nine amino acid residues (Figures 5A and S1). In our structure, the hydrophobic residues in this insert are well-defined and form the ψ-site-2 that binds to Phe823 at the −4 position of the Par-3 peptide. We predicted that this aPKC unique insertion is likely to play a role in the substrate specificities of the kinases. To test this, we deleted the 9-residue insertion ("IVGSSDNPD," Figure S1) from PKCι, and the mutant kinase lost its binding capacity to

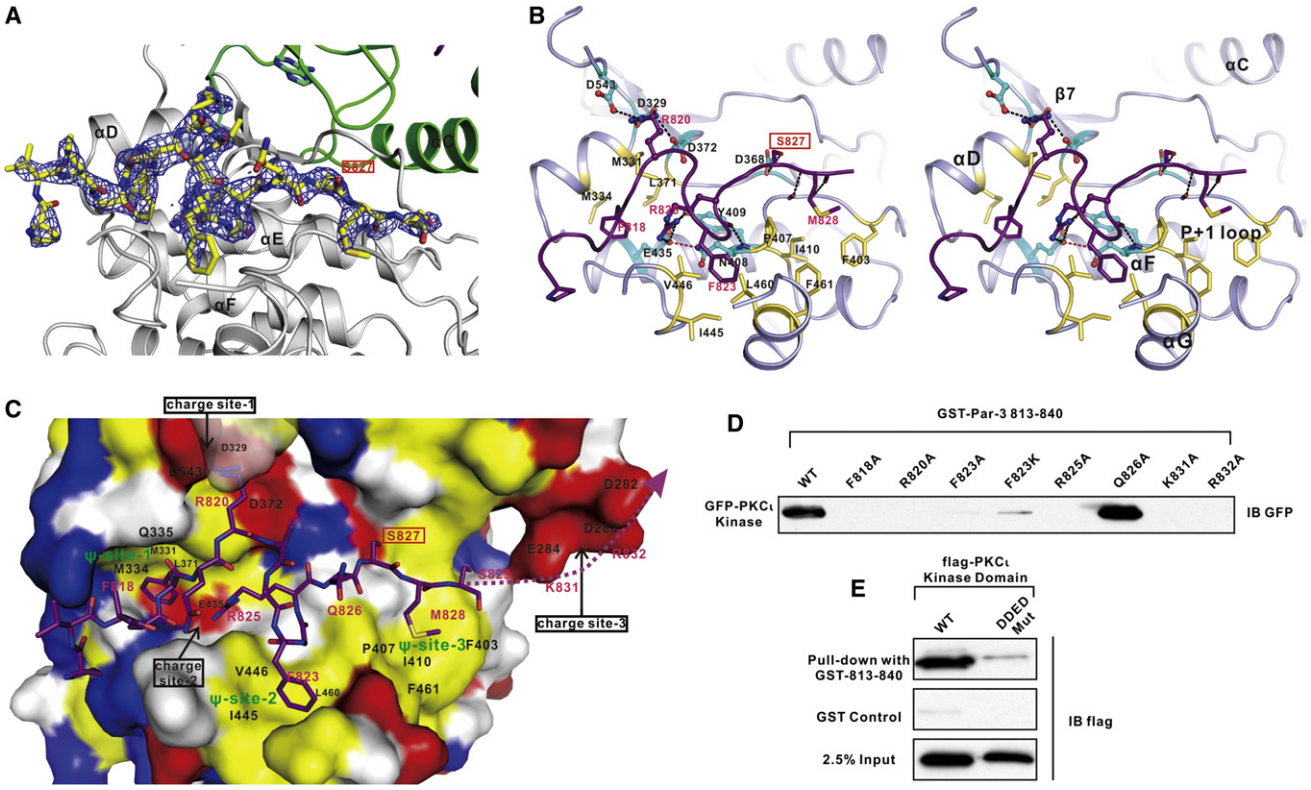

Figure 4. The Interaction Surface between PKCι and the Par-3 Peptide

(A) The omit map of the Par-3 peptide in the PKCι/Par-3 structure. The kinase N-lobe and C-lobe are colored in green and gray, respectively. The Par-3 peptide is colored in yellow. The Fo-Fc density map is shown in blue and contoured at 3σ.

(B) Stereo-view of the PKCι/the Par-3 peptide interface. The backbone of the Par-3 peptide and its side chains interacting with PKCι are shown in purple. The hydrophobic and charged residues from PKCι, which are involved in the interaction with Par-3, are drawn in yellow and cyan, respectively.

(C) The combined surface (PKCι) and stick (Par-3) representations of the PKCι/the Par-3 peptide interface. The positively charged residues of PKCι are drawn in blue, the negatively charged residues in red, the hydrophobic residues in yellow and the others in gray. The residues C-terminal to Ser829 of the Par-3 peptide and the ^{282}DDED^{285} -segment of PKCι could not be seen in our crystal structure. The ^{282}DDED^{285} -segment in this drawing is modeled onto the PKCι structure based on the structure of PKCι in complex with an inhibitor (PDB code: 3A8X). The three hydrophobic sites and the three charged sites, which are key contacting sites with the Par-3 peptide, are indicated.

(D) Mutational analysis of the roles of selected residues from the Par-3 peptide in binding to PKCι.

(E) Substitution of the ^{282}DDED^{285}-segment in PKCι with the corresponding sequence from PKA ("KLQK") largely decreases its binding to Par-3.

See also Figure S1.

the Par-3 peptide (Figure 5C). Additionally, at the edge of the ψ-site-2 of aPKC is a strictly conserved Asn (Asn408 in PKCι). The corresponding residue in other ABC kinases including cPKC and nPKC is a negatively charged Asp/Glu (Figure S1). It is predicted that the presence of a negatively charged residue instead of Asn408 would hinder the hydrophobic interaction between Phe823 of Par-3 and the ψ-site-2 of the kinase (Figure 5A). Indeed, substitution of Asn408 with Asp weakened PKCι's binding to Par-3 (Figure 5C). Similarly, removal of the turn-2 of Par-3 (^{821}EGFG^{824}) essentially eliminated Par-3's binding to PKCι (Figure 5D, top row). We tested this Par-3 deletion mutant in its possible binding to *Drosophila* eye-PKC, which is a member of cPKC. It was found that this Par-3 mutant displayed a slightly enhanced binding to eye-PKC when compared to the WT Par-3 (Figure 5D, bottom row), as if the mutation had converted the Par-3 peptide to be a better cPKC substrate.

Pseudosubstrate of aPKC Regulates Substrate Binding and Phosphorylation

The PKC family kinases are known to possess a pseudosubstrate (PS) right before the C1 domain. The PS sequences of PKCs resemble their substrate sequences but has an Ala residue at the 0 position instead of a Ser/Thr (Pearce et al., 2010). The predicted PS of PKCι is located immediately N-terminal to the C1 domain, and aligns well with the Par-3 peptide (Figure 6A). The difference between PS and the Par-3 peptide is that PS does not have a hydrophobic residue that is equivalent to Phe823 of the Par-3 peptide, thus this PS binds to the kinase domain of PKCι with a weaker affinity than the Par-3 peptide does (Figure 6B). Nonetheless, because PS binding to the kinase domain in the full-length PKCι is an intramolecular interaction, the binding is expected to be considerably stronger than the intermolecular interaction shown in Figure 6B.

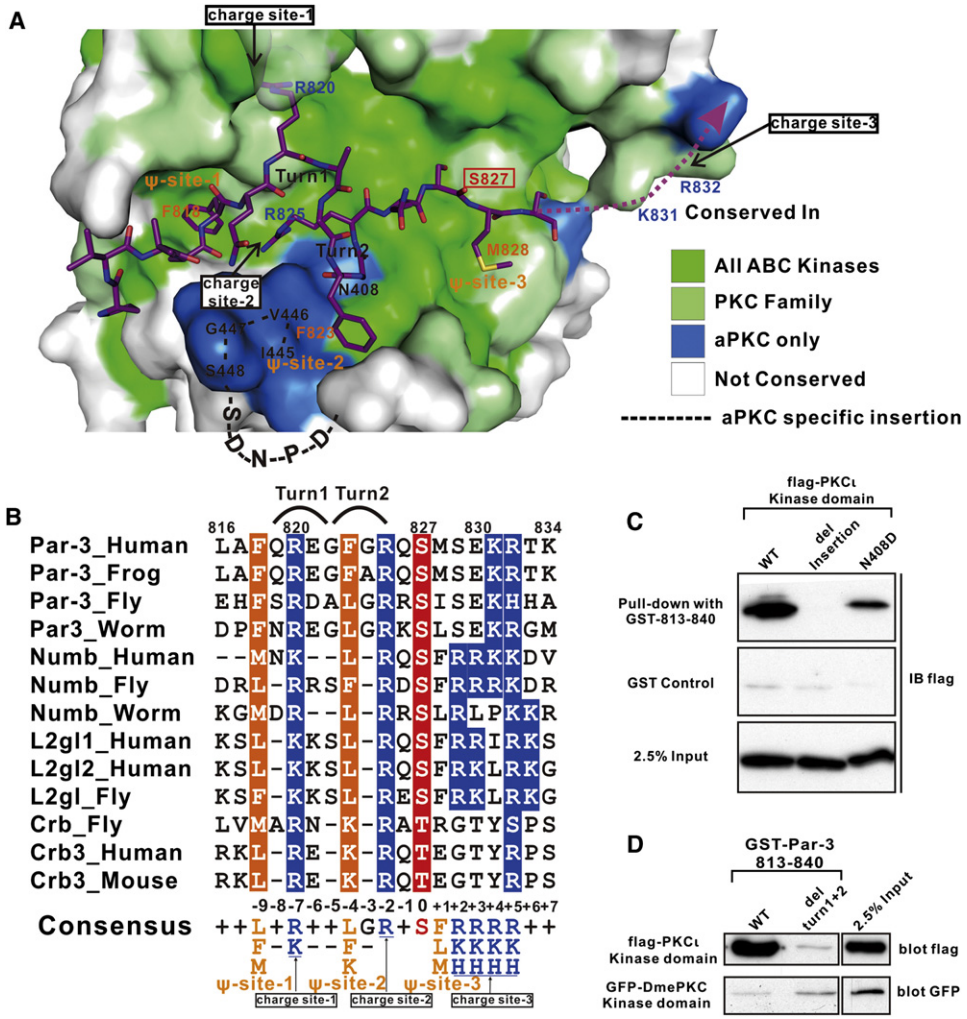

Figure 5. A Consensus Substrate Recognition Motif of aPKCs

(A) The amino acid conservation map of the residues in the substrate binding grooves of ABC kinases including PKA, PKB, and PKC isozymes drawn on the surface of the PKCι structure. Residues that are totally conserved in all ABC kinases are shown in green, those conserved only in the PKC subfamily are shown in light green, the aPKC-specific residues are shown in blue, and nonconserved residues are in gray. A stretch of five residues in the unique aPKC insert ("SDNPD") that are not defined in the crystal structure is indicated and connected with a dashed line.

(B) Structural based sequence alignment of reported aPKC's substrates. The positions of residues N- and C-terminal to the phosphorylation site Ser/Thr are indicated at the bottom of the alignment. The consensus sequence motif derived from the alignment is also included at the bottom of the alignment. The interaction sites of the consensus residues on the kinase domain are indicated below the alignment.

(C) Deletion of the aPKC specific insertion residue forming the ψ-site-2 disrupts PKCι's binding to Par-3. Substitution of Asn408 in the ψ-site-2 with Asp also weakens PKCι's binding to Par-3.

(D) Removal of ^{821}EGFG^{824} from the Par-3 reduces its binding to PKCι. In contrast, removal of ^{821}EGFG^{824} from the Par-3 slightly increased its binding to *Drosophila* eye-PKC.

See also Figure S1.

We tested the functional role of PS in the kinase activity regulation by substituting its "YRR"-cassette with triple Ala residues (Figure 6A). Although not as strong as the kinase domain only of PKCι does, the "YRR/AAA" mutant of the full length kinase displayed a considerably stronger binding to the Par-3 peptide than the wild-type full length enzyme (Figure 6C), indicating that the autoinhibition of the kinase is largely relived in the mutant. We further demonstrate that the "YRR/AAA" mutant of the full length PKCι displayed a higher kinase activity than the wild-type kinase in phosphorylating Par-3 (Figure 6D), further supporting that the PS sequence indeed inhibits the kinase activity of PKCι by blocking the accessibility of kinase's real substrates. Finally, amino acid sequence analysis of other members of the PKC subfamily kinases reveals that all PKCs contain similar pseudosubstrate motifs (Figure 6E).

DISCUSSION

The PKCι/Par-3 complex structure solved in this work represents, to our knowledge, the first substrate-bound form structure

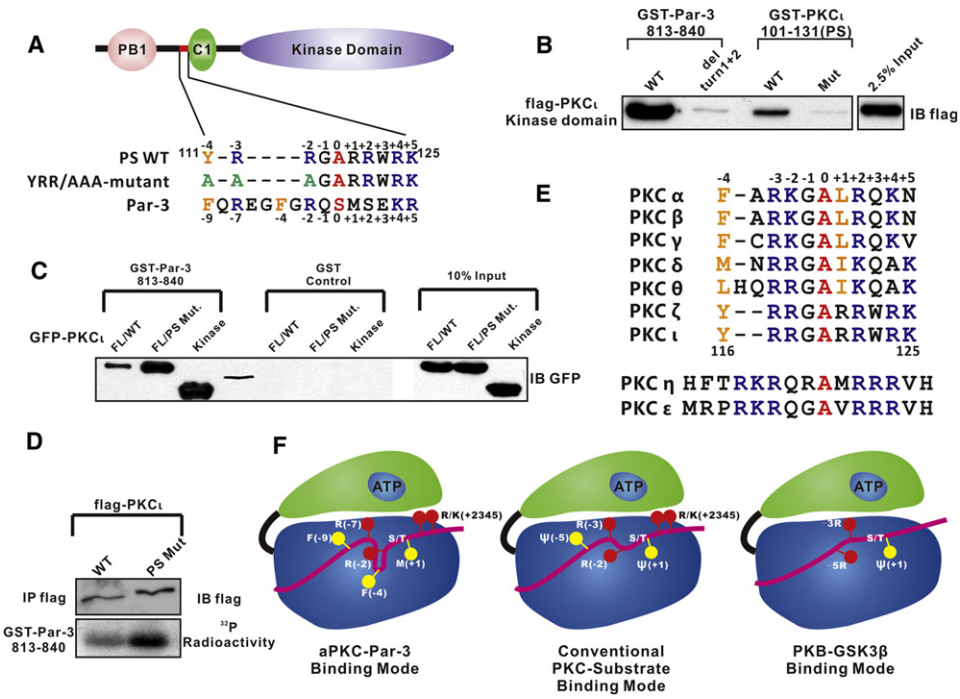

Figure 6. The Pseudosubstrate Sequence Binds to and Inhibits the Kinase Activity of PKCι

(A) Schematic diagram showing the domain organization and the sequence of the pseudosubstrate of PKCι.

(B) The pseudosubstrate (PS) of PKCι binds to the kinase domain with a lower affinity than that of the Par-3 peptide does. Mutations of the "YRR"-cassette at the −4 to −2 position of PS with triple Ala eliminates the binding between the kinase domain and PS of PKCι. Note that the blot in this panel is the same as the one shown in the top panel of Figure 5D.

(C) PS inhibits the binding between PKCι and Par-3. The Par-3 peptide shows a much weaker binding affinity to the full-length PKCι than to the kinase domain of PKCι. Release of the auto-inhibition with the "YRR/AAA"-mutation enhances PKCι's binding to Par-3.

(D) The PS inhibits the kinase activity of PKCι. Release of the autoinhibition with the "YRR/AAA"-mutation enhances PKCι's kinase activity in phosphorylating Par-3.

(E) Structure-based sequence alignment of the PS sequences in PKC isozymes.

(F) A schematic diagram summarizing the substrate binding modes of the ABC family kinases. The figure depicts that the ABC family kinases share overlapping substrate recognition patterns. However, the presence of specific hydrophobic binding pockets for recognizing bulky hydrophobic residues upstream of Ser/Ter(0) distinguishes aPKCs from other kinases.

See also Figure S1.

of the PKC family isozymes. In the complex, PKCι adopts a closed, catalytically competent conformation. The PKCι/Par-3 complex structure also reveals that neither the Par-3 substrate peptide binding nor the formation of the active conformation seems to require phosphorylation of Thr402 in the activation loop of the kinase. The extensive interactions of the residues from the activation loop with both lobes of the kinase domain are sufficient to define the conformation of the activation loop. Phosphorylation of Thr402 does not induce significant conformational changes of the activation loop or the kinase domain of PKCι as a whole (Figure 3B). The PKCι/Par-3 complex structure also reveals that Leu394 in the activation loop interacts extensively with Phe422 at the beginning of αF of the kinase domain (Figure 3B). The presence a Phe at the first residue of αF is unique to aPKCs and PKCδ. The corresponding residue in the rest of ABC family kinases either a positively charged residue or Pro (Figure S1). This structure- and sequence-based analysis nicely explains why aPKC and PKCδ do not require the activation loop phosphorylation for their kinase activities (Stempka et al., 1997; Ranganathan et al., 2007). The finding that aPKCs do not require their activation loop for their kinase activities has important functional implications. For example, unlike other members of PKC isozymes, activities of aPKCs do not require them to be primed by other kinases such as PDK1. Instead, regulated spatial localizations of aPKCs are known to be critically important for their cellular functions (Betschinger et al., 2003; Smith et al., 2007). Consistent with this notion, functions of aPKC in numerous Par-3/Par-6/aPKC-mediated cellular processes are not known to require another upstream kinase to phosphorylate its activation loop.

The atomic structure of the PKCι/Par-3 complex, together with previously solved structures of various ABC family kinases (Yang et al., 2002; Zheng et al., 1993) allows us to better define their substrate specificities. The surface conservation map of the substrate binding groove of the ABC family kinases clearly shows that all these kinases share a common set of substrate binding pockets including two charge sites (charge sites 1 and 2) (Figure 5A). Therefore, the ABC family kinases share certain common features in the sequences of their substrates. For example, all prefer to have two positively charged amino acids

N-terminal to the phosphorylation site (Figure 6F). The similarities of the substrate binding grooves among PKC subfamily isozymes are even higher (Figure 5A), therefore their substrates overlapping is also expected to be higher, as they all contains an extra charge site 3. Nonetheless, aPKCs contain a unique hydrophobic site (ψ-site-2, Figures 4C and 5A), which is absent in cPKCs and nPKCs. Thus, aPKCs prefer substrates with an additional bulky hydrophobic residue sandwiched by two positively charged residues in their sequences N-terminal to Ser/Thr(0) (Figure 6F).

EXPERIMENTAL PROCEDURES

Antibodies

Mouse Anti-GFP antibody was purchased from Santa Cruz; mouse anti-flag antibody M2 was from Sigma-Aldrich.

GST Pull-Down Assay

HEK293T cells transiently transfected with various GFP-PKCι or flag-PKCι encoding plasmids were harvested at 18 hr posttransfection. Collected cells were lysed using the lysis buffer (50 mM HEPES, 150 mM NaCl, 100 mM NaF, 1% Triton X-100, 10% glycerol, 1.5 mM $MgCl_2$, 1 mM EGTA, 1 mM DTT, 0.5 mM PMSF, 10 mM PNPP, 20 mM β-glycerolphosphate, 50 μM sodium vanadate, and a cocktail of protease inhibitors from Calbiochem). In each binding reaction, 0.15 nmol of purified GST-fused Par-3 protein and 100 μl GFP-PKCι-containing cell lysates were mixed in 900 μl PBS. The mixture was incubated at 4°C for 30 min before being centrifuged at 14,000 × g for 5 min. The supernatant was mixed with 25 μl of fresh GSH-coupled Sepharose 4B slurry beads and the mixture was incubated for another 30 min. After two times washing with the wash buffer (with 0.1% Triton X100, otherwise same as the lysis buffer), the proteins captured by the GSH-Sepharose beads were boiled and resolved with SDS-PAGE. GFP-PKCι or flag-PKCι captured by GST-Par-3 was immunodetected using corresponding antibody.

Protein Expression and Purification

The kinase dead kinase domain of mouse PKCι (aa 222–586 with Lys273 substituted Arg; GenBank accession code: BC021630.1) was cloned into the pFastBac HTB vector (from Invitrogen) using the EcoRI single restriction digestion site. The recombinant virus was obtained by transposition and transfection following the Bac-to-Bac expression system's user manual and serial amplified by infecting sf-9 cells of increasing volumes. For expression, 300 ml of sf-9 cells (~1 × 10^6 cells per mL) was infected by virus with multiplicity of infection value of 10, and cells were collected by centrifugation at 400 × g after 72 hr incubation at 27°C. Collected cells were resuspended in the Ni^{2+}-NTA affinity column binding buffer (5 mM imidazole, 500 mM NaCl, 50 mM Tris, 2 mM β-mercaptoethanol, pH 8.5) with a cocktail of protease inhibitors from Calbiochem and then lysed by sonication. The soluble portion of the cell lysate was obtained by centrifugation at 30,000 × g and loaded onto a Ni^{2+}-NTA affinity column. After 30 min incubation, the column was washed extensively with the wash buffer (the column buffer plus 30 mM imidazole). The captured, His-tagged PKCι was eluted with 6 ml elution buffer (the column buffer plus 1 M imidazole) and further purified by another step of size exclusion chromatography (S200 column from GE Healthcare) in the final buffer (50 mM Tris, 100 mM NaCl, 1 mM DTT, and 1 mM EDTA, pH 8.0).

In Vitro Kinase Assay

HEK293T cells transfected with the flag-tagged wide type or mutant PKCι kinase domain was lysed using the lysis buffer. Approximately 100 μl cell lysate was mixed with 400 μl PBS, 1 μg M2 anti-flag antibody, and 25 μl protein G beads slurry. The mixture was incubated at 4°C for 2 hr. The protein G beads-captured PKCι was washed twice with the lysis buffer and then once with the kinase assay buffer (20 mM MOPS, 100 mM NaCl, 15 mM $MgCl_2$, 100 μM ATP, pH 7.2). The antibody-captured PKCι was released by the addition of the flag peptide to a final concentration of 0.1 mg/ml. In each kinase reaction assay, ~20 μg GST-Par-3 was mixed with PKCι in 50 μl of the kinase assay buffer containing 0.2 μCi [γ-P^{32}]-ATP, and the reaction was allowed to proceed for 30 min at room temperature before being terminated with boiling. The proteins in the reaction mixtures were separated by SDS-PAGE. The SDS-PAGE gel was dried and the phosphorylated GST-Par-3 proteins were detected by autoradiography.

Crystallization, Data Collection, and Processing

Crystals of the K273R-PKCι kinase domain in complex with the Par-3 peptide were obtained by the hanging drop vapor diffusion method at 16°C. The freshly purified protein at a concentration of 8 mg/ml was mixed with 5 mM $MgCl_2$, 200 μM AMPPCP, and five times molar ratio of the Par-3 peptide. The PKCι/Par-3 complex crystals were grown in 3.5 M sodium formate, pH7.0. The crystal was quickly frozen by dipping into liquid nitrogen. X-ray data were collected at the beam-line BL17U1 of the Shanghai Synchrotron Radiation Facility. The diffraction data were processed and scaled by HKL2000 (Otwinowski and Minor, 1997).

Using the structure of the aPKC kinase domain (PDB id: 1ZRZ) as the search model, the initial structural model was solve using the molecular replacement method in PHASER (McCoy et al., 2007). The model was then refined by the phenix.refinement (Adams et al., 2010). COOT (Emsley and Cowtan, 2004) was used for peptide modeling and model adjustments. TLS refinement was applied at the final refinement stage. The final structure was validated by phenix.model_vs_data validation tool (Adams et al., 2010). The structure figures were prepared using the program PyMOL (http://pymol.sourceforge.net/).

ACCESSION NUMBERS

The atomic coordinates of PKCι/Par-3 complex structure have been deposited to the Protein Data Bank under the accession code 4DC2.

SUPPLEMENTAL INFORMATION

Supplemental Information includes three figures and can be found with this article online at doi:10.1016/j.str.2012.02.022.

ACKNOWLEDGMENTS

We thank the BL17U1 beamline of the Shanghai Synchrotron Radiation Facility for the X-ray beamline time. This work was supported by the Research Grants Council of Hong Kong (663808, 664009, 660709, 663610, 663811, HKUST6/CRF/10, SEG_HKUST06, and AoE/M-04/04 to M.Z.). C.W., Y.S., and J.Y. performed experiments; C.W., Y.S., and M.Z. designed experiments, analyzed data, and wrote the article; M.Z. coordinated the project. M.Z. is a senior fellow of the Institute for Advanced Study of HKUST.

Received: December 3, 2011
Revised: February 24, 2012
Accepted: February 27, 2012
Published: May 8, 2012

REFERENCES

Adams, J.A. (2003). Activation loop phosphorylation and catalysis in protein kinases: is there functional evidence for the autoinhibitor model? Biochemistry *42*, 601–607.

Adams, P.D., Afonine, P.V., Bunkóczi, G., Chen, V.B., Davis, I.W., Echols, N., Headd, J.J., Hung, L.W., Kapral, G.J., Grosse-Kunstleve, R.W., et al. (2010). PHENIX: a comprehensive Python-based system for macromolecular structure solution. Acta Crystallogr. D Biol. Crystallogr. *66*, 213–221.

Behn-Krappa, A., and Newton, A.C. (1999). The hydrophobic phosphorylation motif of conventional protein kinase C is regulated by autophosphorylation. Curr. Biol. *9*, 728–737.

Betschinger, J., Mechtler, K., and Knoblich, J.A. (2003). The Par complex directs asymmetric cell division by phosphorylating the cytoskeletal protein Lgl. Nature *422*, 326–330.

Emsley, P., and Cowtan, K. (2004). Coot: model-building tools for molecular graphics. Acta Crystallogr. D Biol. Crystallogr. *60*, 2126–2132.

Etienne-Manneville, S., and Hall, A. (2003). Cell polarity: Par6, aPKC and cytoskeletal crosstalk. Curr. Opin. Cell Biol. *15*, 67–72.

Fields, A.P., and Regala, R.P. (2007). Protein kinase C iota: human oncogene, prognostic marker and therapeutic target. Pharmacol. Res. *55*, 487–497.

Goode, N., Hughes, K., Woodgett, J.R., and Parker, P.J. (1992). Differential regulation of glycogen synthase kinase-3 beta by protein kinase C isotypes. J. Biol. Chem. *267*, 16878–16882.

Grodsky, N., Li, Y., Bouzida, D., Love, R., Jensen, J., Nodes, B., Nonomiya, J., and Grant, S. (2006). Structure of the catalytic domain of human protein kinase C beta II complexed with a bisindolylmaleimide inhibitor. Biochemistry *45*, 13970–13981.

Hao, Y., Du, Q., Chen, X., Zheng, Z., Balsbaugh, J.L., Maitra, S., Shabanowitz, J., Hunt, D.F., and Macara, I.G. (2010). Par3 controls epithelial spindle orientation by aPKC-mediated phosphorylation of apical Pins. Curr. Biol. *20*, 1809–1818.

Henrique, D., and Schweisguth, F. (2003). Cell polarity: the ups and downs of the Par6/aPKC complex. Curr. Opin. Genet. Dev. *13*, 341–350.

Herget, T., Oehrlein, S.A., Pappin, D.J.C., Rozengurt, E., and Parker, P.J. (1995). The myristoylated alanine-rich C-kinase substrate (MARCKS) is sequentially phosphorylated by conventional, novel and atypical isotypes of protein kinase C. Eur. J. Biochem. *233*, 448–457.

House, C., and Kemp, B.E. (1987). Protein kinase C contains a pseudosubstrate prototype in its regulatory domain. Science *238*, 1726–1728.

Johnson, D.A., Akamine, P., Radzio-Andzelm, E., Madhusudan, M., and Taylor, S.S. (2001). Dynamics of cAMP-dependent protein kinase. Chem. Rev. *101*, 2243–2270.

Kalive, M., Faust, J.J., Koeneman, B.A., and Capco, D.G. (2010). Involvement of the PKC family in regulation of early development. Mol. Reprod. Dev. *77*, 95–104.

Kornev, A.P., Taylor, S.S., and Ten Eyck, L.F. (2008). A helix scaffold for the assembly of active protein kinases. Proc. Natl. Acad. Sci. USA *105*, 14377–14382.

Le Good, J.A., Ziegler, W.H., Parekh, D.B., Alessi, D.R., Cohen, P., and Parker, P.J. (1998). Protein kinase C isotypes controlled by phosphoinositide 3-kinase through the protein kinase PDK1. Science *281*, 2042–2045.

Leonard, T.A., Różycki, B., Saidi, L.F., Hummer, G., and Hurley, J.H. (2011). Crystal structure and allosteric activation of protein kinase C βII. Cell *144*, 55–66.

Martiny-Baron, G., and Fabbro, D. (2007). Classical PKC isoforms in cancer. Pharmacol. Res. *55*, 477–486.

McCoy, A.J., Grosse-Kunstleve, R.W., Adams, P.D., Winn, M.D., Storoni, L.C., and Read, R.J. (2007). Phaser crystallographic software. J. Appl. Cryst. *40*, 658–674.

Messerschmidt, A., Macieira, S., Velarde, M., Bädeker, M., Benda, C., Jestel, A., Brandstetter, H., Neuefeind, T., and Blaesse, M. (2005). Crystal structure of the catalytic domain of human atypical protein kinase C-iota reveals interaction mode of phosphorylation site in turn motif. J. Mol. Biol. *352*, 918–931.

Morais-de-Sá, E., Mirouse, V., and St. Johnston, D. (2010). aPKC phosphorylation of Bazooka defines the apical/lateral border in Drosophila epithelial cells. Cell *141*, 509–523.

Nagai-Tamai, Y., Mizuno, K., Hirose, T., Suzuki, A., and Ohno, S. (2002). Regulated protein-protein interaction between aPKC and PAR-3 plays an essential role in the polarization of epithelial cells. Genes Cells *7*, 1161–1171.

Newton, A.C. (1997). Regulation of protein kinase C. Curr. Opin. Cell Biol. *9*, 161–167.

Newton, A.C. (2003). Regulation of the ABC kinases by phosphorylation: protein kinase C as a paradigm. Biochem. J. *370*, 361–371.

Nishikawa, K., Toker, A., Johannes, F.J., Songyang, Z., and Cantley, L.C. (1997). Determination of the specific substrate sequence motifs of protein kinase C isozymes. J. Biol. Chem. *272*, 952–960.

Otwinowski, Z., and Minor, W. (1997). Processing of X-ray diffraction data collected in oscillation mode. Methods Enzymol. *276*, 307–326.

Pearce, L.R., Komander, D., and Alessi, D.R. (2010). The nuts and bolts of AGC protein kinases. Nat. Rev. Mol. Cell Biol. *11*, 9–22.

Ponting, C.P., and Parker, P.J. (1996). Extending the C2 domain family: C2s in PKCs delta, epsilon, eta, theta, phospholipases, GAPs, and perforin. Protein Sci. *5*, 162–166.

Prehoda, K.E. (2009). Polarization of Drosophila neuroblasts during asymmetric division. Cold Spring Harb. Perspect. Biol. *1*, a001388.

Ranganathan, S., Wang, Y., Kern, F.G., Qu, Z., and Li, R. (2007). Activation loop phosphorylation-independent kinase activity of human protein kinase C zeta. Proteins *67*, 709–719.

Smith, C.A., Lau, K.M., Rahmani, Z., Dho, S.E., Brothers, G., She, Y.M., Berry, D.M., Bonneil, E., Thibault, P., Schweisguth, F., et al. (2007). aPKC-mediated phosphorylation regulates asymmetric membrane localization of the cell fate determinant Numb. EMBO J. *26*, 468–480.

Sotillos, S., Díaz-Meco, M.T., Caminero, E., Moscat, J., and Campuzano, S. (2004). DaPKC-dependent phosphorylation of Crumbs is required for epithelial cell polarity in Drosophila. J. Cell Biol. *166*, 549–557.

Stempka, L., Girod, A., Müller, H.J., Rincke, G., Marks, F., Gschwendt, M., and Bossemeyer, D. (1997). Phosphorylation of protein kinase Cdelta (PKCdelta) at threonine 505 is not a prerequisite for enzymatic activity. Expression of rat PKCdelta and an alanine 505 mutant in bacteria in a functional form. J. Biol. Chem. *272*, 6805–6811.

Suzuki, A., Akimoto, K., and Ohno, S. (2003). Protein kinase C lambda/iota (PKClambda/iota): a PKC isotype essential for the development of multicellular organisms. J. Biochem. *133*, 9–16.

Takimura, T., Kamata, K., Fukasawa, K., Ohsawa, H., Komatani, H., Yoshizumi, T., Takahashi, I., Kotani, H., and Iwasawa, Y. (2010). Structures of the PKC-iota kinase domain in its ATP-bound and apo forms reveal defined structures of residues 533-551 in the C-terminal tail and their roles in ATP binding. Acta Crystallogr. D Biol. Crystallogr. *66*, 577–583.

Tan, S.L., and Parker, P.J. (2003). Emerging and diverse roles of protein kinase C in immune cell signalling. Biochem. J. *376*, 545–552.

Taylor, S.S., and Kornev, A.P. (2011). Protein kinases: evolution of dynamic regulatory proteins. Trends Biochem. Sci. *36*, 65–77.

Wagner, J., von Matt, P., Sedrani, R., Albert, R., Cooke, N., Ehrhardt, C., Geiser, M., Rummel, G., Stark, W., Strauss, A., et al. (2009). Discovery of 3-(1H-indol-3-yl)-4-[2-(4-methylpiperazin-1-yl)quinazolin-4-yl]pyrrole-2,5-dione (AEB071), a potent and selective inhibitor of protein kinase C isotypes. J. Med. Chem. *52*, 6193–6196.

Webb, B.L., Hirst, S.J., and Giembycz, M.A. (2000). Protein kinase C isoenzymes: a review of their structure, regulation and role in regulating airways smooth muscle tone and mitogenesis. Br. J. Pharmacol. *130*, 1433–1452.

Xu, Z.B., Chaudhary, D., Olland, S., Wolfrom, S., Czerwinski, R., Malakian, K., Lin, L., Stahl, M.L., Joseph-McCarthy, D., Benander, C., et al. (2004). Catalytic domain crystal structure of protein kinase C-theta (PKCtheta). J. Biol. Chem. *279*, 50401–50409.

Yang, J., Cron, P., Good, V.M., Thompson, V., Hemmings, B.A., and Barford, D. (2002). Crystal structure of an activated Akt/protein kinase B ternary complex with GSK3-peptide and AMP-PNP. Nat. Struct. Biol. *9*, 940–944.

Zheng, J., Trafny, E.A., Knighton, D.R., Xuong, N.H., Taylor, S.S., Ten Eyck, L.F., and Sowadski, J.M. (1993). 2.2 A refined crystal structure of the catalytic subunit of cAMP-dependent protein kinase complexed with MnATP and a peptide inhibitor. Acta Crystallogr. D Biol. Crystallogr. *49*, 362–365.